Numerical Continuation in Classical Mechanics and Thermodynamics

Journal:	*European Journal of Physics*
Manuscript ID:	EJP-100348.R4
Manuscript Type:	Paper
Date Submitted by the Author:	n/a
Complete List of Authors:	Gimenez, Aleix; Universitat Politecnica de Catalunya, Chausse, Victor; Universitat Politecnica de Catalunya, Meseguer, Alvaro; Universitat Politecnica de Catalunya, Applied Physics
Article Keywords:	Numerical methods, Nonlinear systems, Arclength continuation
Abstract:	In this paper, modern numerical continuation methodologies are presented as a way of understanding and computing multiplicity of solutions in undergraduate physics problems. Mechanical and thermodynamical problems are used as a storyline to introduce the mathematical formalism required to make clear the distinction between uniqueness and multiplicity of equilibrium solutions and critical states of a nonlinear physical problem as well as to illustrate how these novel numerical continuation techniques are implemented in practice. The paper provides simple numerical Matlab codes easily adaptable to other problems as well as updated software and literature resources currently available.

Numerical Continuation in Classical Mechanics and Thermodynamics

Aleix Gimenez and Victor Chausse

Escola Tècnica Superior d'Enginyeria de Telecomunicació de Barcelona (ETSETB)

Universitat Politècnica de Catalunya

Edifici B3-Ricardo Valle Campus Nord Jordi Girona, 1-3 08034 Barcelona (Spain)

Alvaro Meseguer*

Department of Applied Physics, Universitat Politècnica de Catalunya

B5 Campus Nord Jordi Girona, 1-3 08034 Barcelona (Spain)

(Dated: September 11, 2014)

Abstract

In this paper, modern numerical continuation methodologies are presented as a way of understanding and computing multiplicity of solutions in undergraduate physics problems. Mechanical and thermodynamical problems are used as a storyline to introduce the mathematical formalism required to make clear the distinction between uniqueness and multiplicity of equilibrium solutions and critical states of a nonlinear physical problem as well as to illustrate how these novel numerical continuation techniques are implemented in practice. The paper provides simple numerical MATLAB codes easily adaptable to other problems as well as updated software and literature resources currently available.

I. INTRODUCTION

Numerical continuation methods are a very powerful tool to understand the concept of multiplicity or nonuniqueness of solutions in nonlinear physics[1]. In academic physics courses, it is not always sufficiently emphasized that, for a prescribed set of external conditions, a given nonlinear physical problem may exhibit multiple solutions such as *equilibria* or *critical states*. During the last four or five decades, nonlinearity in the physics literature has become the rule, not the exception. Concepts such as *chaos*, *bifurcation points* (sometimes also termed as *tipping points*) have progressively appeared with more frequency. Whereas chaos and *bifurcation theory* have already reached their maturity[2] as a new branch of mathematical physics, its inclusion in undergraduate academic books is still in its early stage, being generally relegated to non-compulsory material and always addressed from a qualitative point of view. One of the reasons of this limited scope of nonlinear problems in undergraduate syllabuses is the student's lack of a basic numerical analysis background. Nonlinearity and chaos are frequently introduced to undergraduates by means of simple low-dimensional dynamical systems such as double pendulums or logistic maps[3–5]. From a pedagogical point of view, these types of physical models contain the essential ingredients to visualize chaotic dynamics, requiring only very basic mathematical and numerical methodologies to formulate and approximate them, respectively. However, the analysis of the aforementioned problems is frequently focused on their dynamical aspects rather than on the underlying topological structure of the state space, characterized by the equilibrium solutions or critical points.

Bifurcations (i.e. topological changes in parameter-dependent phase spaces) lie at the very heart of chaotic dynamics. In nonlinear systems, these type of dynamics require multiplicity of equilibria. The first step to be taken when studying a nonlinear system is the exploration of the families of fixed points or critical solutions when parameters are varied. Numerical continuation methods are designed precisely for that purpose, i.e., tracking families of solutions of the nonlinear system as a function of some parameter, as well as monitoring their analyticity properties. The concept of parameter-dependent solutions can be extended to general nonlinear systems of algebraic equations in many branches of physics, ranging from optics and chemical kinetics to fluid dynamics.

A proper understanding of the concept of nonuniqueness of solutions in classical and modern physics requires new approaches, both analytical and numerical, not only to shed

light on the underlying mechanisms responsible for the emergence of multiple solutions in nonlinear problems, but also to accurately predict their presence in parameter-dependent systems. From the theoretical point of view, the Implicit Function Theorem, henceforth termed as IFT, plays a crucial role in the required conditions that may give rise to the presence or absence of solutions. In academic environments, the enormous implications of the IFT regarding the existence and uniqueness of solutions in mathematical physics problems are not always properly stressed.

There are many excellent monographs on continuation methods available in the literature. However, these texts are usually intended for a more advanced audience, ranging from graduate students to specialized researchers. Our attempt in this work is to approach the undergraduate student to the concepts of algebraic nonlinearity and parametric dependence from a mathematical and numerical point of view by using a more academic style. The analysis presented here pursues rigorous and detailed formulation of the mathematical problem combined with the application of highly accurate state of the art numerical continuation methodologies. Although the techniques shown here are applicable to systems arising in many branches of nonlinear physics, we focus on two academic problems in mechanics (the double rotating pendulum) and thermodynamics (study of phase transitions of real gases) the student is already familiar with. The problems have been chosen for the sake of clarity, not for their particular complexity, thus allowing a straightforward mathematical formulation, as well as accurate and computationally efficient numerical implementation. With the two examples shown, it is our goal to illustrate how nonlinearity appears in many branches of physics and how a deep mathematical understanding of the nonlinear algebraic problem at hand can be addressed with universal methodologies.

Other mechanical problems, such as the stability of fluid flows or elastic media, could have been treated using numerical continuation methods[6]. However, addressing these problems would require from the student to have a strong mathematical background in the theory of partial differential equations and numerical linear algebra. These topics are typically taught at a graduate or master level and are out of the scope of undergraduate audiences.

The paper is structured as follows. Section II is devoted to the mathematical and numerical formulation of continuation problems. This section also illustrates some of the concepts with a mechanical example that can be addressed analytically. Section III applies the numerical algorithms to a mechanical problem similar to the one analyzed in Section II but

where numerical methods are needed, whereas IV applies the same techniques within the framework of undergraduate thermodynamics. Finally, Appendix A outlines the MATLAB codes used to solve the aforementioned problems.

II. MATHEMATICAL AND NUMERICAL FORMULATION

The mathematical formulation that leads to the determination of equilibrium or critical solutions of parameter-dependent physical problems generally boils down to systems of nonlinear equations. These equations may have an algebraically explicit expression but in some cases, as we will see later, it is not always possible to write these equations in closed form. In any case, we consider a system of n nonlinear equations with n variables $\mathbf{x} = (x_1, x_2, \ldots, x_n)$ and one parameter[7] α:

$$\begin{aligned} F_1(x_1, x_2, \ldots, x_n, \alpha) &= 0 \\ F_2(x_1, x_2, \ldots, x_n, \alpha) &= 0 \\ &\vdots \\ F_n(x_1, x_2, \ldots, x_n, \alpha) &= 0. \end{aligned} \tag{1}$$

In a more compact fashion, the system of equations above can be written as $\mathbf{F}(\mathbf{x}, \alpha) = 0$, with $\mathbf{x} \in \mathbb{R}^n$, $\alpha \in \mathbb{R}$ and $\mathbf{F} : \mathbb{R}^{n+1} \longrightarrow \mathbb{R}^n$. We can think of $\mathbf{x}$ as the set of physical variables that describe a certain state of the system (position coordinates, angles, current intensities in a circuit, thermodynamic pressure or volume of a gas in equilibrium, etc.) whereas α plays the role of an external forcing or condition that acts on the system such as an oscillatory frequency imposed by a signal generator, an environtmental temperature, etc.

Assume that, for some prescribed value of the external parameter $\alpha = \alpha^0$, our physical system exhibits an equilibrium state $\mathbf{x}^0 = (x_1^0, x_2^0, \ldots, x_n^0)$. That is, $(\mathbf{x}^0, \alpha^0) = (x_1^0, x_2^0, \ldots, x_n^0, \alpha^0)$ satisfies the system of equations (1). A natural question is how this solution changes under small variations of the parameter α, i.e., whether there exist nearby qualitatively similar solutions $\mathbf{x} = \mathbf{x}^0 + \Delta\mathbf{x}$ when the parameter is slightly changed to $\alpha = \alpha^0 + \Delta\alpha$, with $|\Delta\alpha|$ small . The answer to this question is provided by the IFT that states that for those nearby solutions to exist, a necessary condition is for the *jacobian* of $\mathbf{F}$

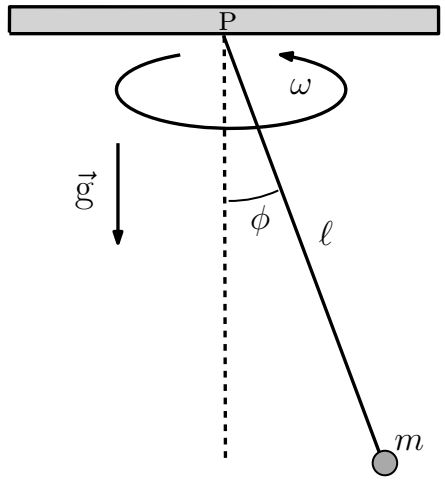

FIG. 1. Rotating pendulum

at $(\mathbf{x}^0, \alpha^0)$ to be a non-singular matrix[8], i.e.:

$$\left|\begin{array}{cccc} \partial_{x_1}F_1 & \partial_{x_2}F_1 & \cdots & \partial_{x_n}F_1 \\ \partial_{x_1}F_2 & \partial_{x_2}F_2 & \cdots & \partial_{x_n}F_2 \\ \vdots & \vdots & & \vdots \\ \partial_{x_1}F_n & \partial_{x_2}F_n & \cdots & \partial_{x_n}F_n \end{array}\right|_{(x^0,\alpha^0)} \neq 0. \tag{2}$$

If condition (2) is satisfied, the IFT guarantees the existence of a *unique* local map $\mathbf{x} = \mathbf{x}(\alpha)$ in a neighbourhood of $(\mathbf{x}^0, \alpha^0)$ satisfying $\mathbf{x}(\alpha^0) = \mathbf{x}^0$. In that case, it is said that system (1) locally defines $\mathbf{x}$ as a *unique implicit function* $\mathbf{x}(\alpha)$ in a neighborhood of the parameter value $\alpha = \alpha^0$.

A. Non-uniqueness of equilibrium solutions: an analytical example

We illustrate some of the concepts previously seen by means of the academic problem of the rotating pendulum. Consider a pendulum consisting of a small marble of mass m attached to a massless rigid rod of length ℓ. The rod-marble system is suspended under the effects of gravity from a fixed point P and is forced to rotate with a constant angular speed $\omega > 0$ around a vertical axis passing through P (see Fig. 1). The purpose of this problem is to find the equilibrium angle ϕ such that the pendulum remains stationary in a frame rotating with angular speed ω. The equilibrium conditions are reduced to the system of

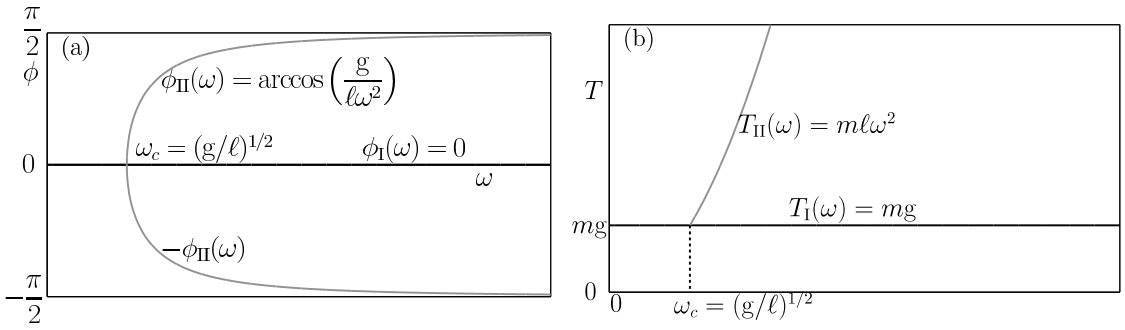

FIG. 2. Families of equilibrium solutions for the rotating pendulum. (a) shows ϕ as a function of ω. (b) shows T as a function of ω.

nonlinear equations involving T (the rod's tension) and ϕ (the equilibrium angle):

$$\left.\begin{aligned} T\cos\phi &= m{\rm g} \\ T\sin\phi &= m\ell\omega^2\sin\phi \end{aligned}\right\}. \tag{3}$$

Therefore the original system (3) is formally written as:

$$\left.\begin{aligned} F_1(T,\phi,\omega) &= 0 \\ F_2(T,\phi,\omega) &= 0 \end{aligned}\right\}, \quad \text{with} \quad \left.\begin{aligned} F_1(T,\phi,\omega) &= T\cos\phi - m{\rm g} \\ F_2(T,\phi,\omega) &= \sin\phi(T - m\ell\omega^2) \end{aligned}\right\}. \tag{4}$$

The question is whether the system (4) defines explicitly T and ϕ as unique functions of the external forcing ω. System (4) offers two different families of solution branches:

- Solution branch (I): $(T,\phi,\omega) = (m{\rm g}, 0, \omega)$, valid for all $\omega > 0$.
- Solution branch (II): $(T,\phi,\omega) = (m\ell\omega^2, \arccos({\rm g}/\ell\omega^2), \omega)$, valid for all $\omega \geq \left(\frac{\rm g}{\ell}\right)^{1/2}$.

Figure 2 shows the two families of equilibrium solutions parametrized as a function of the angular speed ω. For $\omega < \omega_c$, the only available equilibrium solution is branch I: $(\phi_{\rm I}, T_{\rm I}) = (0, m{\rm g})$. Branch II is born at a critical frequency $\omega_c = ({\rm g}/\ell)^{1/2}$. Beyond ω_c, three equilibrium solutions coexist for the same frequency: $\phi_{\rm I}(\omega)$, $\phi_{\rm II}(\omega)$ and its symmetric counterpart, $-\phi_{\rm II}(\omega)$, due to the reflection symmetry of the problem. At $\omega = \omega_c$, the uniqueness of solutions is lost, and this can be identified *a priori* by testing the full-rank condition (2). A straightforward calculation leads to the jacobian of the system (4):

$$DF = \begin{pmatrix} \partial_T F_1 & \partial_\phi F_1 \\ \partial_T F_2 & \partial_\phi F_2 \end{pmatrix} = \begin{pmatrix} \cos\phi & -T\sin\phi \\ \sin\phi & (T - m\ell\omega^2)\cos\phi \end{pmatrix}, \tag{5}$$

with determinant

$$|DF(T,\phi,\omega)| = T - m\ell\omega^2\cos^2\phi.$$

Along branch I, this determinant adopts the value

$$|DF|_{\rm I} \equiv |DF(T_{\rm I},\phi_{\rm I},\omega)| = m(\mathrm{g}-\ell\omega^2), \tag{6}$$

whereas along branch II

$$|DF|_{\rm II} \equiv |DF(T_{\rm II},\phi_{\rm II},\omega)| = m\ell\omega^2\left(1-\frac{\mathrm{g}^2}{\ell^2\omega^4}\right). \tag{7}$$

For $\omega=\omega_c=(\mathrm{g}/\ell)^{1/2}$, $|DF|_{\rm I}=|DF|_{\rm II}=0$, and uniqueness of solutions in a neighborhood of that critical frequency is lost, as expected. The critical frequency ω_c is the only root for both determinants and therefore both branches are locally unique for all $\omega>\omega_c$ so no new solutions are expected to be born from them.

B. Newton's Method and Numerical Continuation

Typically, for an arbitrary value of the parameter $\alpha=\alpha^0$, the possible solution(s) or state(s) $\mathbf{x}^0$ of system (1) are unknown. In general, system (1) for the n-unknowns $x_1,x_2,\ldots,x_n$ has to be solved numerically for $\alpha=\alpha^0$ by means of a suitable algorithm such as the *Newton-Raphson* method[9] given by the iterative formula

$$\mathbf{x}^{(k+1)} = \mathbf{x}^{(k)} - \left(D\mathbf{F}_0^{(k)}\right)^{-1}\mathbf{F}_0^{(k)}, \quad k=0,1,2,\ldots, \tag{8}$$

where $\mathbf{x}^{(k)}=(x_1^{(k)},x_2^{(k)},\ldots,x_n^{(k)})$ is the k-th iterate of the method, $\mathbf{F}_0^{(k)}=\mathbf{F}(\mathbf{x}^{(k)},\alpha^0)$ and $(D\mathbf{F}_0^{(k)})^{-1}$ stands for the inverse of the jacobian matrix $(D\mathbf{F}_0)_{ij}=\partial_{x_j}F_i(\mathbf{x},\alpha^0)$ evaluated at $\mathbf{x}=\mathbf{x}^{(k)}$. In practice, many software packages allow the user to provide the Jacobian analytically. If that option is not possible, the numerical package approximates the Jacobian via finite differences. The codes developed for this work make use of a 2nd order centered finite difference approximation given by the expression

$$\partial_{x_j}F_i\,|_{\mathbf{x}} \approx [F_i(\mathbf{x}+h\mathbf{e}_j)-F_i(\mathbf{x}-h\mathbf{e}_j)]/(2h), \tag{9}$$

where $\mathbf{e}_j$ is the j-th canonical vector and $h\approx 10^{-8}$ in double precision arithmetic[9]. This formula provides a truncation error of order $O(h^2)$.

The iteration must be started from an initial guess $\mathbf{x}^{(0)}$ that must be close to the sought solution $\mathbf{x}^0$ in order to have convergence, i.e., $\lim_{k\to\infty}\mathbf{x}^{(k)} = \mathbf{x}^0$. In that case, the method converges quadratically[10], i.e., $\|\mathbf{x}^{(k+1)} - \mathbf{x}^{(k)}\| < K\,\|\mathbf{x}^{(k)} - \mathbf{x}^{(k-1)}\|^2$, for some positive constant K. Choosing random initial guesses may lead to non-convergent iterations or, in some cases, convergence to other solutions different from the sought state $\mathbf{x}^0$.

The general purpose of continuation techniques is to provide reliable numerical methodologies to track the solutions of (1) when the parameter α is varied.

Here we outline one of the more frequently used continuation algorithms in nonlinear physics: the *Pseudo-Arclength Continuation*, henceforth referred as PAC[1]. In what follows, we define the state vector $\mathbf{y} = (y_1, \ldots, y_n, y_{n+1}) \equiv (x_1, \ldots, x_n, \alpha)$ replacing the original variables of the problem since, as we will see later, the natural continuation parameter α will not always be the right variable to track solutions. In that sense, it is better to think of all the variables as potential continuation parameters. Consider a solution branch manifold M in $\mathbb{R}^{n+1}$ implicitly defined by the n-dimensional nonlinear system of equations

$$\begin{aligned} F_1(y_1, \ldots, y_n, y_{n+1}) &= 0 \\ F_2(y_1, \ldots, y_n, y_{n+1}) &= 0 \\ &\vdots \\ F_n(y_1, \ldots, y_n, y_{n+1}) &= 0. \end{aligned} \tag{10}$$

The coordinates of M can be implicitly parametrized by means of an arc-parameter s, i.e., $\mathbf{y} = \mathbf{y}(s)$. The PAC algorithm is designed to obtain a numerically accurate discrete set of points $\{\mathbf{y}^1, \mathbf{y}^2, \ldots, \mathbf{y}^k, \ldots\} \approx \{\mathbf{y}(s_1), \mathbf{y}(s_2), \ldots, \mathbf{y}(s_k), \ldots\}$ along M by applying suitable predictor and corrector methods. Figure 3a shows a two-dimensional projection of a prototypical continuation manifold $M \subset \mathbb{R}^{n+1}$. Assume $\mathbf{y}^k$ is known, i.e., for $k = 1$ for instance, this can be accomplished by using the Newton method formerly described applied to system (10) for the particular value of the parameter $\alpha^1 = y^1_{n+1}$. The predictor stage provides a first approximation $\widetilde{\mathbf{y}}^{k+1}$ along the tangent direction of M at $\mathbf{y}^k$ dictated by the unitary tangent vector $\widehat{\mathbf{v}}^k$ (see Fig. 3b). At any arbitrary point $\mathbf{y}(s) \in M$, this vector can be computed by implicit differentiation of system (10) with respect to the arc-parameter s leading to the

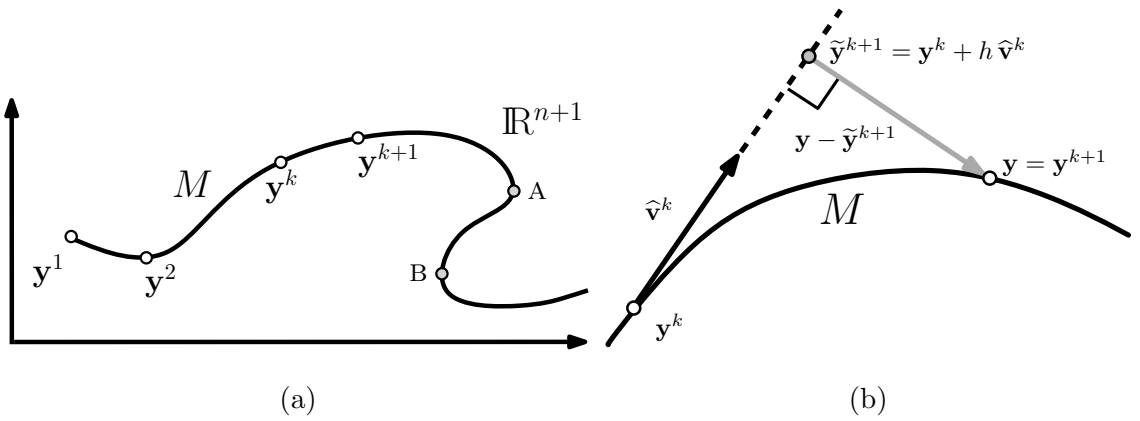

(a) (b)

FIG. 3. (a) Two-dimensional projection of a generic manifold $M \subset \mathbb{R}^{n+1}$ implicitly defined by system (10). (b) Geometrical representation of the PAC algorithm: tangent predictor $\widetilde{\mathbf{y}}^{k+1}$ and normal corrector solution $\mathbf{y}^{k+1}$ of the auxiliar appended system (14).

homogeneous overdetermined system of equations

$$\begin{bmatrix} \partial_{y_1} F_1 & \cdots & \partial_{y_{n+1}} F_1 \\ \partial_{y_1} F_2 & \cdots & \partial_{y_{n+1}} F_2 \\ \vdots & & \vdots \\ \partial_{y_1} F_n & \cdots & \partial_{y_{n+1}} F_n \end{bmatrix} \begin{bmatrix} v_1 \\ \vdots \\ v_n \\ v_{n+1} \end{bmatrix} = \begin{bmatrix} 0 \\ 0 \\ \vdots \\ 0 \end{bmatrix}, \tag{11}$$

where $v_j = \dfrac{\mathrm{d}}{\mathrm{d}s} y_j$ are the $n+1$ components of the vector $\mathbf{v} = (v_1, \ldots, v_n, v_{n+1})$ tangent to the manifold M at $\mathbf{y}(s)$. System (11) contains n equations involving the $n+1$ unknown components of $\mathbf{v}$. Since the tangent vector is undetermined up to an arbitrary multiplicative constant, this degeneracy can be eliminated by fixing one of the components of $\mathbf{v}$. The usual practice is to set $v_{i_0} = 1$ by introducing the solution vector $\mathbf{v} = (v_1, \ldots, v_{i_0-1}, 1, v_{i_0+1}, \ldots, v_{n+1})$ so equation (11) now reads

$$\begin{bmatrix} \partial_{y_1} F_1 & \cdots & \partial_{y_{i_0-1}} F_1 & \partial_{y_{i_0+1}} F_1 & \cdots & \partial_{y_{n+1}} F_1 \\ \partial_{y_1} F_2 & \cdots & \partial_{y_{i_0-1}} F_2 & \partial_{y_{i_0+1}} F_2 & \cdots & \partial_{y_{n+1}} F_1 \\ \vdots & & \vdots & \vdots & & \vdots \\ \partial_{y_1} F_n & \cdots & \partial_{y_{i_0-1}} F_n & \partial_{y_{i_0+1}} F_n & \cdots & \partial_{y_{n+1}} F_n \end{bmatrix} \begin{bmatrix} v_1 \\ \vdots \\ v_{i_0-1} \\ v_{i_0+1} \\ \vdots \\ v_{n+1} \end{bmatrix} = - \begin{bmatrix} \partial_{y_{i_0}} F_1 \\ \partial_{y_{i_0}} F_2 \\ \vdots \\ \partial_{y_{i_0}} F_n \end{bmatrix}. \tag{12}$$

The i_0-th component must be chosen such that the resulting matrix appearing in (12) is non-singular and well-conditioned in order to ensure uniqueness of solutions and numerical

stability of the algorithm. This requirement is crucial to avoid failure of the continuation, particularly when the current estimate $\mathbf{y}$ is approaching a bifurcation point. Numerical continuation software packages[11] deal with this problem by computing tangent directions of the bifurcating branches. In the present work we simply avoid these pathological points by starting our continuation algorithm slightly away from the bifurcations.

The *tangent predictor* $\widetilde{\mathbf{y}}^{k+1}$ for the next point $\mathbf{y}^{k+1}$ is obtained by locally approximating M along its tangent direction:

$$\widetilde{\mathbf{y}}^{k+1} = \mathbf{y}^k + h\,\widehat{\mathbf{v}}^k, \tag{13}$$

where h is a suitably small step size (see Fig. 3b) and $\widehat{\mathbf{v}}^k$ is the normalized vector resulting from solving (12). The last stage of the PAC consists in the *correction*. Here we proceed with the simplest version based on solving the auxiliar or appended nonlinear system for the unknown $\mathbf{y} \equiv \mathbf{y}^{k+1}$

$$\begin{bmatrix} F_1(\mathbf{y}) \\ F_2(\mathbf{y}) \\ \vdots \\ F_n(\mathbf{y}) \\ \langle \widehat{\mathbf{v}}^k, \mathbf{y} - \widetilde{\mathbf{y}}^{k+1} \rangle \end{bmatrix} = \begin{bmatrix} 0 \\ 0 \\ \vdots \\ 0 \\ 0 \end{bmatrix}. \tag{14}$$

This $(n+1)$-dimensional nonlinear system is solved with Newton's method using $\mathbf{y}^{(0)} = \widetilde{\mathbf{y}}^{k+1}$ as initial guess. Geometrically, solving system (14) is equivalent to finding $\mathbf{y} \in M$ with $\mathbf{y} - \widetilde{\mathbf{y}}^{k+1}$ orthogonal to the tangent prediction direction (see Fig. 3b).

In this work, we provide simple continuation MATLAB codes that deal with two particular problems in mechanics and thermodynamics. A complete description of the codes (`main.m, continuation.m, examplefun.m` and `graphgenerator.m`) is provided in Appendix A. These codes are just intended to illustrate the continuation techniques introduced here, not as a multipurpose tool for other applications. There are many continuation algorithms currently available, the state of the art probably being the MATCONT[11,12] package developed by W. Govaerts and Yu A. Kuznetsov. This package embraces robust algorithms with many features such as step-size control of h (to avoid extremely small steps and to efficiently deal with turning or saddle-node points) and can identify branching points and tangent directions of new families of solutions emerging from them.

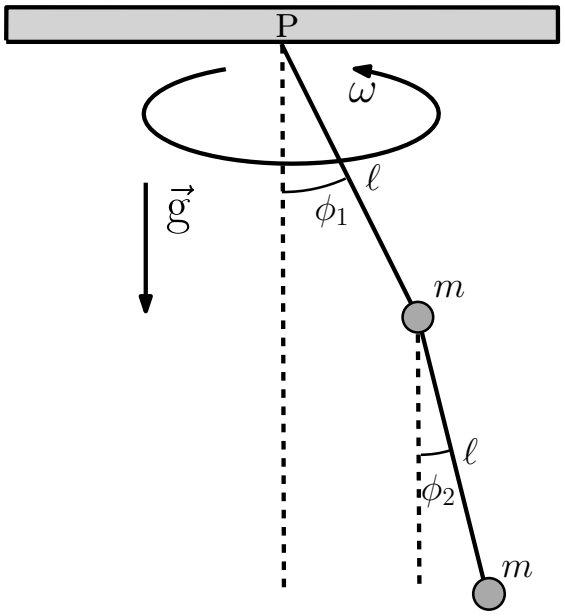

FIG. 4. Double rotating pendulum

III. NUMERICAL CONTINUATION IN MECHANICS

In this section we illustrate a first application of the numerical continuation algorithm to a slightly more complicated problem consisting of a double pendulum with two small spheres of mass m connected by massless rigid rods of equal length ℓ (see Fig. 4). As before, the system is forced to rotate with a constant angular speed ω around the vertical axis. As in the previous section, we are asked for equilibrium solutions in a ω-speed co-rotating frame. Let T_1 and T_2 be the tensions of the upper and lower rod,respectively. Application of Newton's laws for equilibrium leads to:

$$T_1 \sin\phi_1 - T_2 \sin\phi_2 = m\omega^2 \ell \sin\phi_1, \tag{15a}$$

$$T_1 \cos\phi_1 - T_2 \cos\phi_2 = m\,\mathrm{g}, \tag{15b}$$

$$T_2 \sin\phi_2 = m\omega^2 \ell(\sin\phi_1 + \sin\phi_2), \tag{15c}$$

$$T_2 \cos\phi_2 = m\,\mathrm{g}. \tag{15d}$$

Formal substitution of (15c) and (15d) in (15a) and (15b), respectively, leads to the elimination of T_2 from the first two equations:

$$T_1 \sin\phi_1 = m\omega^2 \ell(2\sin\phi_1 + \sin\phi_2), \tag{16a}$$

$$T_1 \cos\phi_1 = 2m\,\mathrm{g}. \tag{16b}$$

For simplicity we only seek equilibria within the domain

$$(\phi_1, \phi_2) \in [0, \pi/2) \times (-\pi/2, \pi/2),$$

bearing in mind that for each solution (ϕ_1, ϕ_2) there exists its symmetric version $(-\phi_1, -\phi_2)$. Quotients between equations (16a)-(16b) and (15c)-(15d) are used to eliminate the tensions from the original system, which is reduced to:

$$\begin{aligned} F_1(\phi_1, \phi_2, \alpha) &= \tan(\phi_1) - \alpha(2\sin\phi_1 + \sin\phi_2) \;=\; 0 \\ F_2(\phi_1, \phi_2, \alpha) &= \tan(\phi_2) - 2\alpha(\sin\phi_1 + \sin\phi_2) \;=\; 0, \end{aligned} \tag{17}$$

where $\alpha = \ell\omega^2/2\mathrm{g}$ is a dimensionless parameter and the functions $\tan(\phi_1)$ and $\tan(\phi_2)$ are well behaved within the search domain. We start by analyzing the trivial solution branch I: $(\phi_1, \phi_2) = (0, 0), \forall\alpha$. In this particular case, the jacobian and its determinant can be calculated analytically, leading to $|DF|_{\mathrm{I}} = 2\alpha^2 - 4\alpha + 1$. Since in this case the determinant is a quadratic polynomial, we expect at most two potential critical situations. This polynomial has roots at $\alpha_\pm = (2 \pm \sqrt{2})/2$, with $\alpha_- \approx 0.293$ and $\alpha_+ \approx 1.707$. At $\alpha = \alpha_-$, branch II (BR-II) is born (dashed curves in Fig. 5a and Fig. 5b). The qualitative properties of BR-II are similar to those corresponding to the single rotating pendulum seen in Section II. Both angles ϕ_1 and ϕ_2 are positive and grow monotonically, eventually stagnating at the asymptotic values $(\phi_1, \phi_2) \to (\pi/2, \pi/2)$. However, the angles ϕ_1 and ϕ_2 are different along BR-II, as shown in Fig. 5c, where the difference $\phi_1 - \phi_2$ is plotted as a function of α. For very small values of α, the difference $\phi_1 - \phi_2$ is remarkable, with a maximum difference $|\phi_1 - \phi_2|_{\max} \approx 0.157$ attained at $\alpha \approx 0.397$ (see inset in Fig. 5c). This discrepancy decreases for higher values of α, being almost indistinguishable to the naked eye for a moderate value of $\alpha = 2$, as shown in Fig. 6a. At $\alpha = \alpha_+$ an unexpected new family (BR-III) of solutions emerges from BR-I with $\phi_1 > 0$ and $\phi_2 < 0$. Along BR-III, ϕ_1 exhibits a rapid growth that attains a maximum value $\phi_1^{\mathrm{m}} \approx 0.6$ at $\alpha_{\mathrm{m}} \approx 3.41$, gray circle in Fig. 5b. For $\alpha > \alpha_{\mathrm{m}}$, this first angle slowly decreases and approaches an asymptotic value $\phi^\infty \approx 0.52$. By contrast, the behaviour of ϕ_2 along BR-III is quite regular and similar, in absolute value, to that observed for ϕ_1 or ϕ_2 in BR-II, approaching an asymptotic value $\phi_2 \to -\pi/2$. Along BR-III, the angles ϕ_1 and ϕ_2 are not symmetrical ($\phi_2 \neq -\phi_1$) as can be seen in Fig. 5d where the quantity $\phi_1 + \phi_2$ is plotted as a function of α.

Monitoring the jacobian of BR-I is crucial for forecasting these new emerging branches that can be continuated by means of sophisticated strategies[11]. In the absence of such techniques,

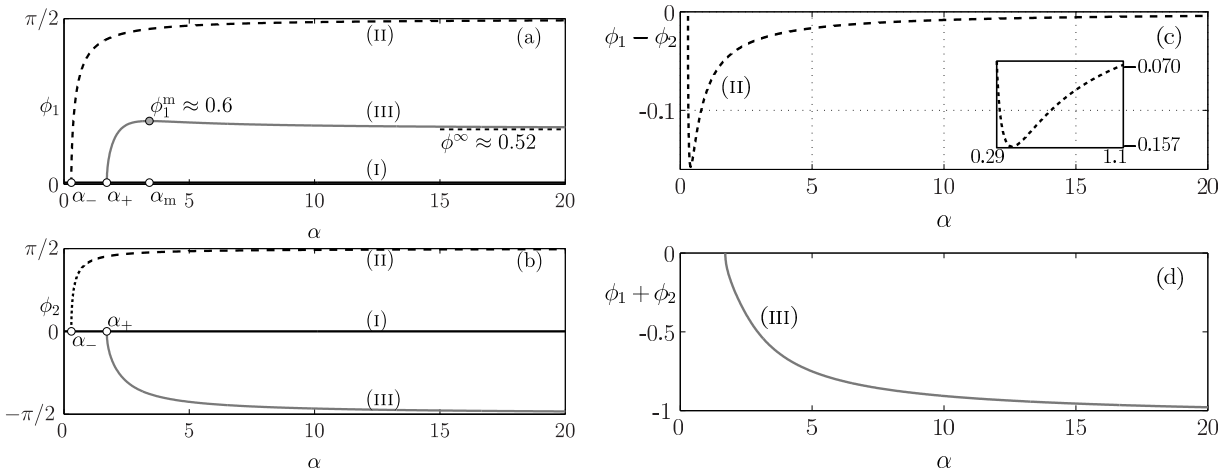

FIG. 5. Families of equilibrium solutions for the double rotating pendulum. (a) ϕ_1. (b) ϕ_2. Their symmetric counterparts $-\phi_1$ and $-\phi_2$ are not represented. (c) Difference $\phi_1 - \phi_2$ along BR-II ; inset shows a detail of the minimum attained at $\alpha \approx 0.397$. (d) Sum of angles $\phi_1 + \phi_2$ along BR-III.

we simply explore the presence of new solutions by inspection, i.e., using Newton's method for $\alpha_- < \alpha < \alpha_+$ or $\alpha > \alpha_+$ to detect BR-II or BR-III, respectively, starting the iteration from different initial guesses until a new solution branch is identified. The jacobian determinant of system (17) has been computed numerically along BR-I, BR-II and BR-III, see Fig. 6b. Along branch BR-I, this determinant becomes zero at $\alpha = \alpha_+$ and $\alpha = \alpha_-$. According to the IFT, the uniqueness of implicit functions must be lost in a neighbourhood of α_+ and α_-. It is precisely at those roots where the jacobian determinant evaluated at the two other branches BR-II and BR-III also vanishes. Away from these two singularities α_- or α_+, the determinants $|DF|_{\mathrm{II}}$ and $|DF|_{\mathrm{III}}$ were always found to be non-zero, thus indicating that both branches do not generate new families of solutions, at least within the range explored $\alpha \in [0, 20]$.

Overall, the families of equilibrium solutions that we have just found constitute the scaffolding that would be crucial if we attempted to understand the dynamical counterpart of the problem. If the double rotating pendulums were allowed to oscillate, these branches of solutions would condition which configuration will be stable or unstable and whether chaotic dynamics are present. However, a dynamical approach to the problem is far from the scope of this study.

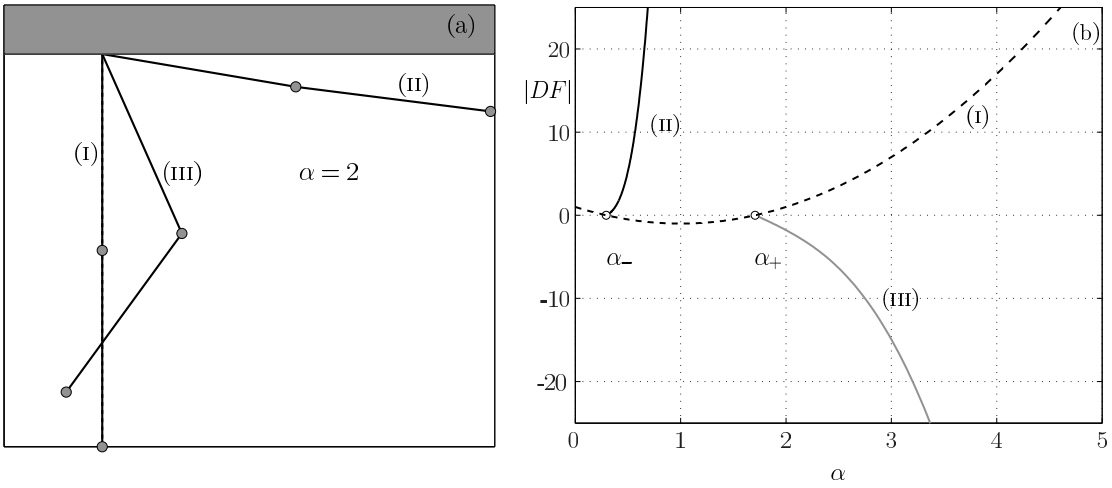

FIG. 6. (a) Geometrical representation of the three possible equilibrium configurations for $\alpha = 2$. (b) Determinant of the jacobian of system (17) evaluated along branches BR-I, BR-II and BR-III. The values α_- and α_+ make the determinant zero.

IV. APPLICATIONS TO PHASE TRANSITIONS IN THERMODYNAMICS

Another application of numerical continuation arises in the study of phase transitions of real gases from the point of view of equilibrium thermodynamics. Isothermal compression of a gas may lead to a liquid-vapour phase transition below a critical temperature, along which the pressure remains constant. Many academic courses and textbooks in thermodynamics address the theoretical study of this phenomena by means of the *van der Waals* equation. However, a similar analysis for the *Dieterici* equation is hard to find. These aforementioned equations describe qualitatively the shape of the isotherms of a real gas and both may describe, to some extent, first order phase transitions.

These equations are particular cases of a more general situation: consider a gas obeying the equation of state

$$p = p(v, T) \tag{18}$$

where p is the pressure, v the molar volume and T the temperature. The mathematical formulation will henceforth be established in *reduced* thermodynamic variables so that the coordinates of the *critical point*[13] satisfying

$$\partial_v p = \partial_v^2 p = 0, \tag{19}$$

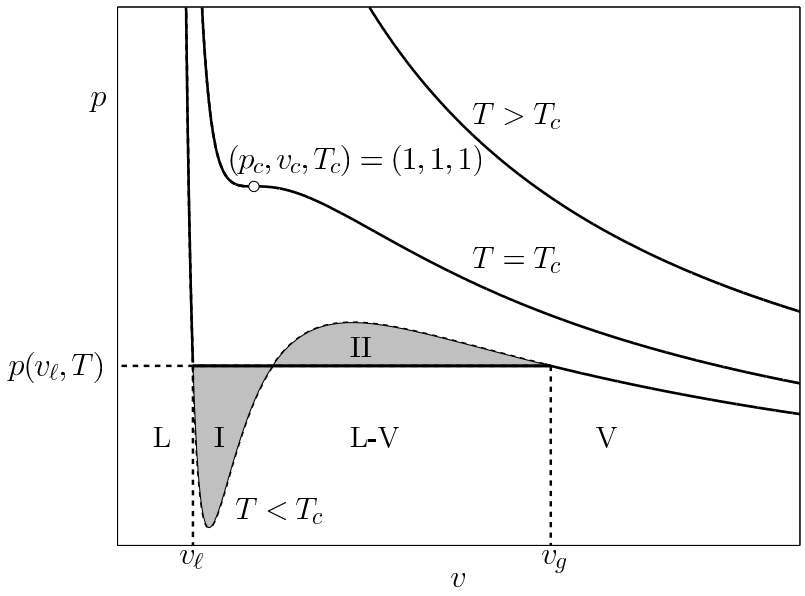

FIG. 7. Lever rule across a generic subcritical isotherm indicating liquid (L), liquid-vapour (L-V) and vapour (V) regions. The white circle is located at the critical point and the pressure at v_g must be $p(v_\ell, T)$.

are:

$$p_c = v_c = T_c = 1.$$

Figure 7 shows three generic supercritical, critical and subcritical isotherms with $T > T_c$, $T = T_c$ and $T < T_c$ in equation (18), respectively. A challenging numerical problem is the computation of the volumes v_ℓ and v_g for an arbitrary subcritical isotherm $T < T_c = 1$. These volumes are obtained by imposing two conditions. The first condition is usually called the *lever rule*, i.e., the shadowed areas of regions I and II of Fig.7 must be equal. For a detailed derivation of this rule we refer the reader to Section 3.4 of Callen's monograph on thermodynamics[13]. The second constraint is that the pressures $p_\ell = p(v_\ell, T)$ and $p_g = p(v_g, T)$ must coincide (see Fig. 7). The two aforementioned conditions lead to the system of equations to be solved:

$$\begin{aligned} F_1(v_\ell, v_g, T) &= \int_{v_\ell}^{v_g} p(v, T)\, \mathrm{d}v - (v_g - v_\ell)\, p(v_\ell, T) = 0 \\ F_2(v_\ell, v_g, T) &= p(v_g, T) - p(v_\ell, T) = 0. \end{aligned} \tag{20}$$

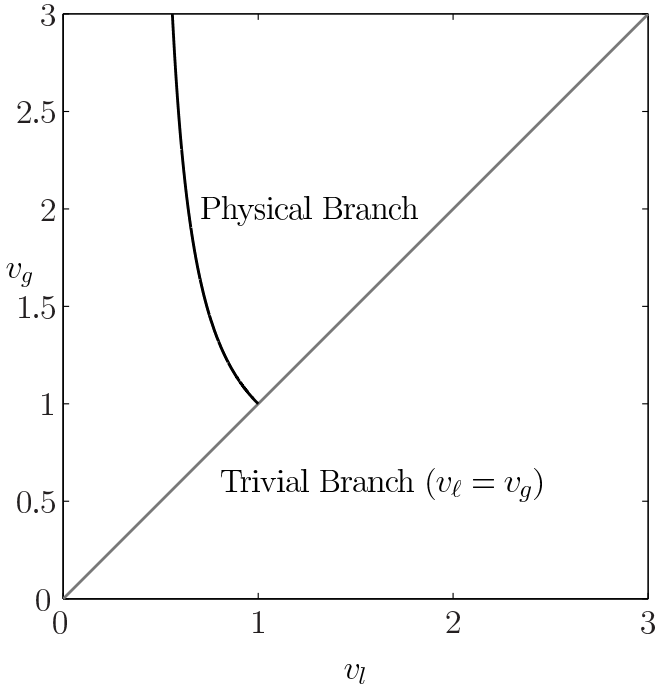

FIG. 8. Physical solution branch (black) emerging from the critical point ($v_\ell = v_g = 1$).

In this case, the jacobian matrix of system (20) is

$$DF = \begin{pmatrix} \partial_{v_l} F_1 & \partial_{v_g} F_1 \\ \partial_{v_l} F_2 & \partial_{v_g} F_2 \end{pmatrix} = \begin{pmatrix} (v_l - v_g)\partial_v p(v_l, T) & p(v_g, T) - p(v_l, T) \\ -\partial_v p(v_\ell, T) & \partial_v p(v_g, T) \end{pmatrix}. \tag{21}$$

System (20) admits the trivial solution $v_l = v_g$, along which the jacobian matrix (21) is rank-deficient with $\text{rank}(DF)_{v_\ell = v_g} = 1$, and therefore singular. According to the IFT, the uniqueness of solutions may be lost along that trivial branch. However, the physically meaningful solution branch is born precisely at the critical point $(v_l, v_g) = (1, 1)$ where the jacobian matrix is identically zero, i. e.: $\partial_v p(1, T) = 0$. The continuation algorithm will successfully identify the physically meaningful sought branch if started locally near that critical point. This situation is illustrated in figure 8 for the van der Waals gas, to be studied in detail in the next section.

A. van der Waals equation

The previous discussion can be applied to the reduced van der Waals equation[14],

$$p(v, T) = \frac{8T}{3v - 1} - \frac{3}{v^2}, \tag{22}$$

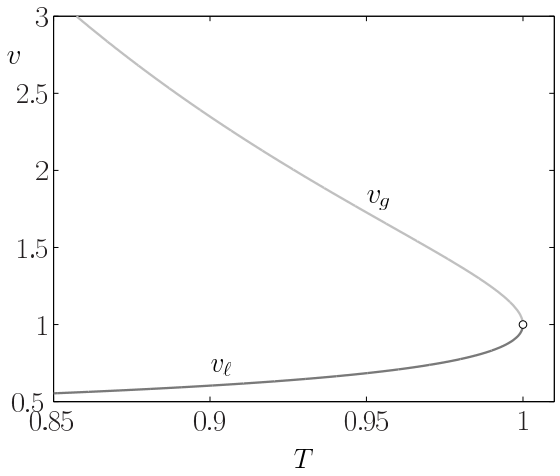

FIG. 9. Two-dimensional projection of coexistence curves v_ℓ (dark gray) and v_g (light gray) as a function of T resulting from the continuation algorithm.

defined for $v > \frac{1}{3}$ and $T > \frac{27}{32}$. In this particular case, the isothermal integration appearing in (20) can be evaluated analytically so that the system can be expressed explicitly in terms of v_ℓ and v_g:

$$\begin{aligned} F_1(v_\ell, v_g, T) &= \log\left(\frac{3v_g-1}{3v_\ell-1}\right) + \frac{9}{4T}\left(\frac{1}{v_g}-\frac{1}{v_\ell}\right) - \frac{1}{3v_g-1} + \frac{1}{3v_\ell-1} = 0 \\ F_2(v_\ell, v_g, T) &= \frac{8T}{3}\left(\frac{1}{3v_g-1}-\frac{1}{3v_\ell-1}\right) - \frac{1}{v_g^2} + \frac{1}{v_\ell^2} = 0. \end{aligned} \tag{23}$$

Figure 9 shows a two-dimensional projection of the coexistence curves $v_\ell(T)$ and $v_g(T)$ resulting from the continuation algorithm applied to system (23) starting near the critical point $(v_\ell, v_g, T) = (1, 1, 1)$ using Newton's method. In this case, both curves are born at the tangent or saddle-node point[1] $T = v = 1$. To avoid convergence to the $v_\ell = v_g$ unphysical solution, the continuation algorithm has to be started slightly away from the critical point $(T < 1)$, and using different values of v_ℓ and v_g as initial guess satisfying $v_\ell < 1 < v_g$. Figure 10a shows the two-dimensional p-v diagram including the solution curves previously shown in Fig. 9. Figure 10b shows a three-dimensional projection of the van der Waals surface along which the coexistence phase region has been shadowed. Finally, Table I contains the coordinates of the coexistence boundaries within the temperature range $T \in [0.85, 1.00]$. The numerical values reported in Table I have been provided with at least 12 significant figures.

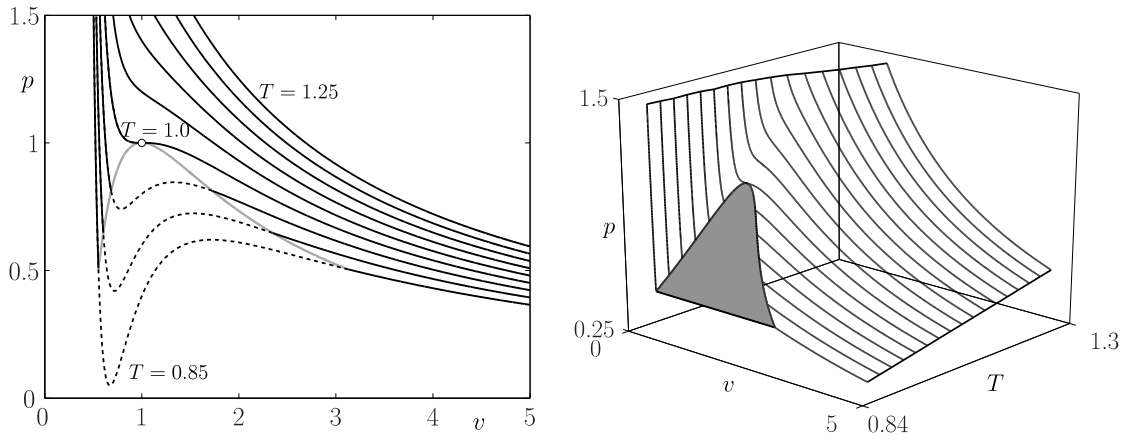

(a) (b)

FIG. 10. (a) Isotherms from van der Waals equation within allowed ranges of temperature. Portions of the isotherms within the interval (v_ℓ, v_g) have been depicted with dashed curves. (b) Three dimensional representation of the $p(v,T)$ surface excluding the transition region (shaded).

T	v_ℓ	v_g	p
1.000	1.000000000000	1.000000000000	1.000000000000
0.975	0.755140600754	1.436931258000	0.902985170975
0.950	0.684122113656	1.727071192256	0.811879243364
0.925	0.637851638159	2.024621393007	0.726585053520
0.900	0.603401903178	2.348842376202	0.646998351872
0.875	0.576016046000	2.712408236896	0.573007253114
0.850	0.553360458440	3.127639292441	0.504491649787

TABLE I. Numerical values of coexistence boundaries for the van der Waals gas.

B. Dieterici equation

The Dieterici equation state in reduced thermodynamic coordinates is[14]:

$$p(v,T) = \frac{T}{2v-1}\exp\left(2 - \frac{2}{vT}\right), \tag{24}$$

with $v > \frac{1}{2}$ due to the finite size of the molecules (similar to the restriction $v > \frac{1}{3}$ in the van der Waals equation). In this case, the integral appearing in F_1 of system (20) cannot be evaluated analytically and must be computed numerically by means of a quadrature formula.

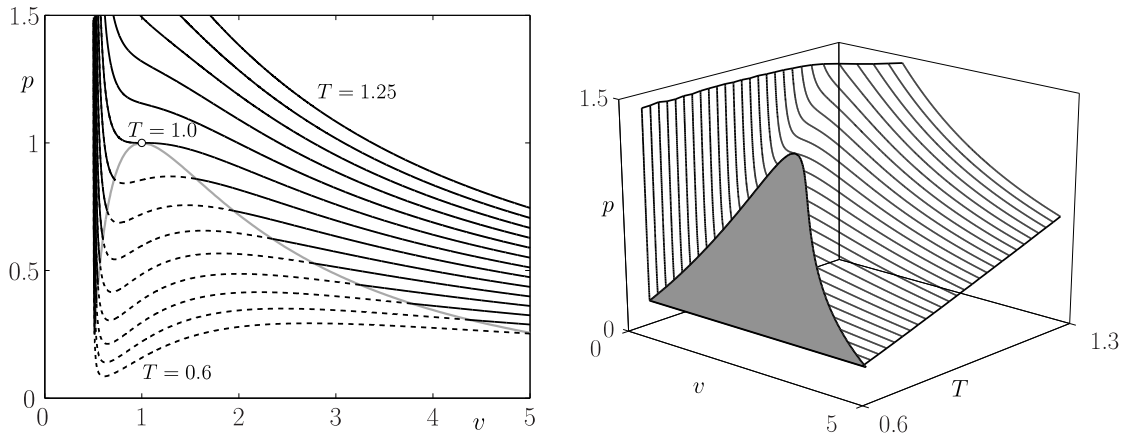

(a) (b)

FIG. 11. (a) Isotherms from Dieterici's equation. Portions of the isotherms within the interval (v_ℓ, v_g) have been depicted with dashed curves. (b) Three dimensional representation of the $p(v,T)$ surface excluding the transition region (shaded).

The system of equations (20) is in this case:

$$\begin{aligned} F_1(v_\ell, v_g, T) &= \mathrm{I}_N(v_\ell, v_g, T) - (v_g - v_\ell)\, p(v_\ell, T) = 0 \\ F_2(v_\ell, v_g, T) &= \frac{1}{2v_g - 1} \exp\left(2 - \frac{2}{v_g T}\right) - \frac{1}{2v_\ell - 1} \exp\left(2 - \frac{2}{v_l T}\right) = 0, \end{aligned} \tag{25}$$

where $\mathrm{I}_N(v_\ell, v_g, T)$ stands for the quadrature approximation of the isothermal integral based on $N+1$ quadrature points $\{v_0, v_1, \ldots, v_N\}$:

$$\mathrm{I}_N(v_\ell, v_g, T) = \sum_{j=0}^{N} w_j\, p(v_j, T), \tag{26}$$

with $\{w_0, w_1, w_2, \ldots, w_N\}$ being the quadrature weights of the formula. Since our purpose is to have a highly accurate evaluation of F_1, we have made use of the *Clenshaw-Curtis* quadrature formula[15]. This quadrature has recently been vindicated as a competitive alternative to classical Gauss formulas[16] since it also provides exponential convergence but with the advantage that the nodes and weights of the corresponding formulas are known explicitly for arbitrary N, overall requiring much less computational cost. The coexistence boundaries resulting from the continuation are summarized in Fig. 11 and also in Table II for $T \in [0.6, 1]$. The reported values in Table II are accurate to 12 decimal places. For the moderate subcritical temperatures used, the number of quadrature nodes required to get the aforementioned accuracy is reasonably low to moderate, with N typically ranging from

T	v_l	v_g	p
1.000	1.000000000000	1.000000000000	1.000000000000
0.975	0.781111623679646	1.35298781861043	0.927216952746984
0.950	0.716033340120983	1.56071003660451	0.858736883359602
0.925	0.673844398915984	1.75463131364776	0.794366307368327
0.900	0.642840743502614	1.94703658154220	0.733915739055988
0.875	0.618652754731553	2.14291782144663	0.677199845628736
0.850	0.599112607104091	2.34511246634668	0.62403760244963
0.825	0.582971832431844	2.55559322308145	0.574252449749519
0.800	0.569440426495074	2.77593847776609	0.527672451399130
0.775	0.557984544445464	3.00754687673802	0.484130456505169
0.750	0.548225305970880	3.25175437322076	0.443464264767860
0.725	0.539883215514119	3.50991026247175	0.405516796684844
0.700	0.532745387783188	3.78343631482155	0.370136269772613
0.675	0.526645096620475	4.07388112954649	0.337176381952146
0.650	0.521448402472000	4.38297702729968	0.306496503042278
0.625	0.517045052448858	4.71270491247043	0.277961874833345
0.600	0.513342069858104	5.06537203109748	0.251443819363877

TABLE II. Numerical values of coexistence boundaries for Dietereci's equation.

26 to 200. However, for small values of T, the lower bound of integration v_ℓ approaches the singular value 1/2, where Dieterici's equation fails to be defined, see Fig. 11a or Table II. As the limit $T \to 0^+$ is approached, the integrand becomes singular at $v = v_\ell$, thus deteriorating the exponential convergence of the quadrature rule. Dealing with this numerical pathology is far beyond the scope of the present work.

V. CONCLUSION

This work illustrates how numerical continuation algorithms can be applied to solve parameter-dependent nonlinear physical equations arising in undergraduate mechanics or thermodynamics courses. The computational techniques required to solve the aforemen-

tioned problems include Newton's method and quadrature formulas for numerical integration. Documented MATLAB codes are included as supplementary material. These codes solve the mechanics and thermodynamics problems exemplified in this work, but they can be adapted for solving similar problems arising in other branches of undergraduate physics.

Appendix A: MATLAB codes

The aim of the codes is to provide the vapour-liquid transition curves for substances obeying van der Waals and Dieterici equations of state, as well as the equilibrium angles for the rotating double pendulum. For the thermodynamics problems, the code provides numerical tables of the coexistence curves with at least 12 correct significant digits. The code is divided in different files that contain functions used by the main script:

- `main.m`: main script.
- `continuation.m`: continuation algorithm.
- `examplefun.m`: M-function to which the continuation is applied.
- `graphgenerator.m`: M-function that provides the figures.

To run the program, copy all the files in a directory and set this folder as MATLAB's working folder. Then type `main` in MATLAB's prompt. The `main` code makes use of function `examplefun.m` which adapts itself to the mechanical or thermodynamical cases by assigning to the global variable `flag` the following values:

- `flag = 1` : Double pendulum.
- `flag = 2` : van der Waals equation.
- `flag = 3` : Dieterici equation.

1. `continuation.m`

   This function performs the pseudo-arclength continuation of the function `fun` from the initial point `y0` and during `maxIt` iterations of step `h`. This function is invoked as follows:

   $$\texttt{yCont} = \texttt{continuation}(\texttt{fun}, \texttt{y0}, \texttt{h}, \texttt{tol}, \texttt{maxIt});$$

   with input arguments:

- `fun`: corresponding to the system (10) satisfying `fun(y)=0`,
- `y=[y1 ... yn yn+1]`: $n+1$ variable array,
- `y0`: starting continuation point,
- `h`: step size,
- `tol`: tolerance of the Newton iteration,
- `maxIt`: total number of iterations,

and output arguments:

- `yCont`: `(n+1)`$\times$`m` matrix with `m=MaxIt` containing:

$$\texttt{yCont} = \begin{bmatrix} y_1^1 & \cdots & y_1^{\texttt{m}} \\ \vdots & & \vdots \\ y_n^1 & \cdots & y_n^{\texttt{m}} \\ y_{n+1}^1 & \cdots & y_{n+1}^{\texttt{m}} \end{bmatrix}.$$

Within `continuation.m`, two inner routines are used:

- `jac.m`: second-order finite difference approximation of the jacobian of an arbitrary vector field $\mathbf{F} : \mathbb{R}^{n+1} \longrightarrow \mathbb{R}^n$. The calling sequence is:

$$\texttt{jacF} = \texttt{jac}(\texttt{fun}, \texttt{y});$$

  where `jacF` is the array containing the Jacobian approximated matrix of function `fun` evaluated at `y`.

- `newtoncorrector.m`: correction to the predictor used in `continuation`. The calling sequence is:

$$\texttt{corr} = \texttt{newtoncorrector}(\texttt{fun}, \texttt{pred}, \texttt{tanVec}, \texttt{tol});$$

  where `fun` is the continuation function, `pred` the current predictor, `tanVec` the tangent vector to the curve at that point and `tol` the tolerance of the Newton iteration. The returning value `corr`, i.e., next continuated point.

2. `examplefun.m`: evaluates the function to perform the continuation and the subroutine `weightCC`, which computes the Clenshaw-Curtis weights of integration (Dietereci's cases) in case `flag=3`. The calling sequence is:

$$\texttt{fun} = \texttt{examplefun}(\texttt{y});.$$

The numerical value of `flag` must be assigned before invoking this function:

- `flag = 1`, the double pendulum approach is taken, and the components of the input variable `y` are: `y(1)` $= \phi_1$, `y(2)` $= \phi_2$ and `y(3)` $= \alpha$. The components of `F` are those explained in the paper.
- `flag = 2`: van der Waals equation is applied. In this case, the components of `y` are: `y(1)` $= v_l$, `y(2)` $= v_g$ and `y(3)` $= T$.
- `flag=3`: Dieterici equation of state is used and no analytic integration can be done. In this case, `weightCC` is called to provide the Clenshaw-Curtis quadrature weights. This subroutine is invoked as follows:

$$\texttt{weights} = \texttt{weightCC}(\texttt{N});$$

This function computes `N` $+ 1$ Clenshaw-Curtis quadrature weights, and stores them in the global variable `weights`.

3. `graphgenerator.m`: The function generates 3 figures:

- ϕ_1 as a function of α.
- ϕ_2 as a function of α.
- two graphics of the isotherms and the coexistence region, for van der Waals and Dieterici, and two tables with the values of T, v_l , v_g and p.

The function has no output arguments, and is called as follows

$$\texttt{graphgenerator}(\texttt{yContII}, \texttt{yContIII}, \texttt{plotVdw}, \texttt{tableVdw}, \texttt{plotD}, \texttt{tableD});$$

where all the input arguments contain the necessary information to generate the figures.

* alvaro.meseguer@upc.edu

[1] Y. A. Kuznetsov, *Elements of Applied Bifurcation Theory*, 3rd edition (Springer-Verlag, New York, 2004).

[2] A. E. Motter and D. K. Campbell, "Chaos at fifty," Phys. Today **66**(5), 27–33 (2013).

[3] T. Shinbrot, C. Grebogi, J. Wisdom and J. A. Yorke,"Chaos in a double pendulum", Am. J. Phys. 60 , 491 (1992)

[4] R. B. Levien and S. M. Tan, "Double pendulum: An experiment in chaos", Am. J. Phys. 61 , 1038 (1993).

[5] J. R. Groff, "Exploring dynamical systems and chaos using the logistic map model of population change". Am. J. Phys. 81 , 725 (2013).

[6] G. Iooss and D. D.Joseph, *Elementary Stability and Bifurcation Theory*, 2nd ed. (Springer Verlag, New York, 1997).

[7] Although we make a clear distinction between the physical variables and the parameter, this categorization will be irrelevant later on when formulating continuation schemes.

[8] J. E. Marsden and M. J. Hoffman, *Elementary Classical Analysis*, 2nd ed. (W.H. Freeman & Company, New York, 1993).

[9] D. Kincaid and W. Cheney, *Numerical Analysis - Mathematics of Scientific Computing*, 3rd edition (Brooks/Cole, Pacific Grove, 2002).

[10] $\|\cdot\|$ stands for the standard Euclidean 2-norm in $\mathbb{R}^n$.

[11] A. Dhooge, W. Govaerts and Yu A. Kuznetsov, ACM TOMS **29**, 141 (2003).

[12] MATCONT Project Web Site, `<http://sourceforge.net/projects/matcont/>`.

[13] H. B. Callen, *Thermodynamics and an introduction to thermostatics*, 2nd ed. (John Wiley and Sons, 1985).

[14] R. J. Sadus, J. Chem. Phys. **115**(3), 1460 (2001).

[15] P. J. Davis, P. Rabinowitz, *Methods of Numerical Integration*, 2nd ed. (Academic Press, Inc. London, 1984).

[16] Trefethen, L. N. , "Is Gauss quadrature better than Clenshaw-Curtis?". SIAM Review 50(1), 67 (2008).